

Nernst effect of iron pnictide and cuprate superconductors: signatures of spin density wave and stripe order

Christian Hess

Abstract The Nernst effect has recently proven a sensitive probe for detecting unusual normal state properties of unconventional superconductors. In particular, it may sensitively detect Fermi surface reconstructions which are connected to a charge or spin density wave (SDW) ordered state, and even fluctuating forms of such a state. Here we summarize recent results for the Nernst effect of the iron pnictide superconductor $\text{LaO}_{1-x}\text{F}_x\text{FeAs}$, whose ground state evolves upon doping from an itinerant SDW to a superconducting state, and the cuprate superconductor $\text{La}_{1.8-x}\text{Eu}_{0.2}\text{Sr}_x\text{CuO}_4$ which exhibits static stripe order as a ground state competing with the superconductivity. In $\text{LaFeAsO}_{1-x}\text{F}_x$, the SDW order leads to a huge Nernst response, which allows to detect even fluctuating SDW precursors at superconducting doping levels where long range SDW order is suppressed. This is in contrast to the impact of stripe order on the normal state Nernst effect in $\text{La}_{1.8-x}\text{Eu}_{0.2}\text{Sr}_x\text{CuO}_4$. Here, though signatures of the stripe order are detectable in the temperature dependence of the Nernst coefficient, its overall temperature dependence is very similar to that of $\text{La}_{2-x}\text{Sr}_x\text{CuO}_4$, where stripe order is absent. The anomalies which are induced by the stripe order are very subtle and the enhancement of the Nernst response due to static stripe order in $\text{La}_{1.8-x}\text{Eu}_{0.2}\text{Sr}_x\text{CuO}_4$ as compared to that of the pseudogap phase in $\text{La}_{2-x}\text{Sr}_x\text{CuO}_4$, if any, is very small.

1 Introduction

The Nernst effect is the generation of a transverse electric field \mathbf{E} upon the application of a magnetic field \mathbf{B} perpendicular to a longitudinal thermal gradient ∇T , i.e., $\mathbf{E} \perp \mathbf{B} \perp \nabla T$. The Nernst *signal* is then defined as the measurable voltage per temperature difference: $e_y = |\mathbf{E}|/|\nabla T| = E_y/|\nabla T|$, and the Nernst *coefficient* is de-

Christian Hess

IFW-Dresden, Institute for Solid State Research, P.O. Box 270116, D-01171 Dresden, Germany,
e-mail: c.hess@ifw-dresden.de

defined as $v = e_y/B$ (see, e.g. [1, 2]). One may relate the Nernst coefficient to other accessible transport quantities through the relation [2, 3]

$$v = \left(\frac{\alpha_{xy}}{\sigma} - S \tan \theta \right) \frac{1}{B}. \quad (1)$$

Here S is the Seebeck coefficient, $\tan \theta$ the Hall angle, σ the electrical conductivity, and α_{xy} the off-diagonal Peltier conductivity. In a one-band metal, the two terms on the right-hand side of Eq. 1 cancel exactly if the Hall angle is independent of energy ('Sondheimer cancellation') [1, 2, 3]. However, in a multiband electronic structure which may arise from the inherent multi-orbital nature of the electronic states at the Fermi level, or from a Fermi surface reconstruction arising in a charge or spin density wave ordered state, this cancellation is no longer valid. The degree of its violation can be determined experimentally by comparing the measured v with the term $S \tan \theta / B$, which can be calculated from electrical resistivity, thermopower, and Hall data.

A little more than ten years ago, the Nernst effect of unconventional superconductors began to attract considerable attention [1, 2, 4, 5, 6, 7, 8, 9, 10, 11, 12, 13, 14]. One reason is that for type-II superconductors it is strongly enhanced by movement of magnetic flux lines (vortices) [15, 16, 17, 18], where the Nernst coefficient v is directly proportional to the drift velocity of the vortices, which has rendered this transport quantity a valuable tool for studying their dynamics. This very fundamental property was used to interpret the unusual enhancement of the Nernst coefficient in the normal state of cuprate high T_c superconductors at temperatures much higher than the critical temperature T_c as the signature of vortex fluctuations [2, 4, 5]. More specifically, it was proposed that in the pseudogap phase above T_c long-range phase coherence of the superconducting order parameter is lost while the pair amplitude remains finite. One more recent proposal to explain an unusual Nernst response in the cuprates was that Fermi surface distortions due to stripe or spin density wave (SDW) order could lead to an enhanced Nernst effect [6, 7, 8, 14]. In particular, for stripe ordering $\text{La}_{1.8-x}\text{Eu}_{0.2}\text{Sr}_x\text{CuO}_4$ and $\text{La}_{1.6-x}\text{Nd}_{0.4}\text{Sr}_x\text{CuO}_4$, an enhanced positive Nernst signal at elevated temperature has been associated with a Fermi surface reconstruction due to stripe order [6]. Furthermore, a strong anisotropy of the Nernst coefficient arising from the broken rotation symmetry of electron-nematic order has been discussed both experimentally and theoretically [9, 10].

SDW order is also an ubiquitous phenomenon in the second class of high temperature superconductors, the iron pnictide superconductors. However, as compared to the cuprates, much less is known about the Nernst effect of this material class. In a pioneering study Zhu et al. reported an anomalous suppression of the off-diagonal thermoelectric current in optimally doped $\text{LaFeAsO}_{1-x}\text{F}_x$ and suggested the presence of SDW fluctuations near the superconducting transition [19]. Matusiak et al. observed a strong enhancement of the Nernst coefficient in the SDW state of the parent compounds and at low doping levels of $\text{CaFe}_{2-x}\text{Co}_x\text{As}_2$ and $\text{EuFe}_{2-x}\text{Co}_x\text{As}_2$, but did not find any particular anomaly in the Nernst effect of a purely superconducting doping level that could be attributed to neither vortex flow nor to SDW fluctuations [20, 21]. Kondrat et al. systematically investigated the doping-evolution of

the Nernst effect in $\text{LaFeAsO}_{1-x}\text{F}_x$ [13]. For the parent compound they observe a huge negative Nernst coefficient accompanied with a severe violation of the Sondheimer cancellation in the SDW state. In their study, a similarly enhanced ν was observed at underdoped ($x = 0.05$) superconducting species, despite the absence of static magnetic order and the presence of bulk superconductivity, strongly suggestive of SDW fluctuations. More conventional transport was observed at optimal doping ($x = 0.1$) where the normal state Nernst signal is rather featureless with a more complete Sondheimer cancellation.

The purpose of this paper is to compare the impact of SDW/stripe ordering phenomena on the Nernst coefficient of respective prototype systems of the iron pnictide and cuprate high-temperature superconductors. For the iron pnictides the focus is on the material $\text{LaFeAsO}_{1-x}\text{F}_x$ which up to present appears to represent the rare case that magnetically ordered and superconducting phases are well separated in the electronic phase diagram [22]. For the cuprates the material under scrutiny is $\text{La}_{1.8-x}\text{Eu}_{0.2}\text{Sr}_x\text{CuO}_4$, which is a prototype system exhibiting stripe order over a wide region of the electronic phase diagram [23]. For each of the considered systems, all considerations and data presented in the next two sections are to a large extent borrowed from two recent studies on $\text{LaFeAsO}_{1-x}\text{F}_x$ and $\text{La}_{1.8-x}\text{Eu}_{0.2}\text{Sr}_x\text{CuO}_4$ by Kondrat et al. [13] and Hess et al. [14], respectively.

2 Nernst effect and SDW fluctuations in the iron-based superconductor $\text{LaFeAsO}_{1-x}\text{F}_x$

In the year 2008, the discovery of superconductivity in $\text{LaFeAsO}_{1-x}\text{F}_x$ [24] initiated a tremendous research effort which yielded soon after a large variety of new superconducting iron pnictide compounds with T_c up to 55 K [25]. Figure 1 reproduces the electronic phase diagram of this compound from reference [22]. The parent compound LaFeAsO is a poor metal and exhibits, as can be inferred from the figure, an antiferromagnetic SDW ground state. The transition towards the SDW state occurs at $T_N = 137$ K and is accompanied by a structural tetragonal-to-orthorhombic transition at $T_s \approx 160$ K [22, 26, 27, 28, 29]. Upon substituting fluorine for oxygen the SDW phase is destabilized, i.e. T_s and T_N gradually decrease and at some finite doping level ($x \lesssim 0.05$) superconductivity emerges. The actual nature of the doping-driven transition from SDW to superconductivity is much under debate. There is evidence that in $\text{LaFeAsO}_{1-x}\text{F}_x$ the transition is abrupt and first order-like towards a homogeneous superconducting state [22] while in other systems (e.g. $\text{SmFeAsO}_{1-x}\text{F}_x$ or $\text{BaFe}_{2-x}\text{Co}_x\text{As}_2$) experiments suggest a finite doping interval where superconductivity and static magnetism coexist [30, 31]. The obvious proximity to antiferromagnetism suggests spin fluctuations being important for the mechanism of superconductivity with a respective impact on the normal state properties, including the normal state transport [13, 28, 32, 33, 34].

The normal state transport properties of the samples from which the phase diagram has been constructed have been studied in great detail [13, 28, 34], where

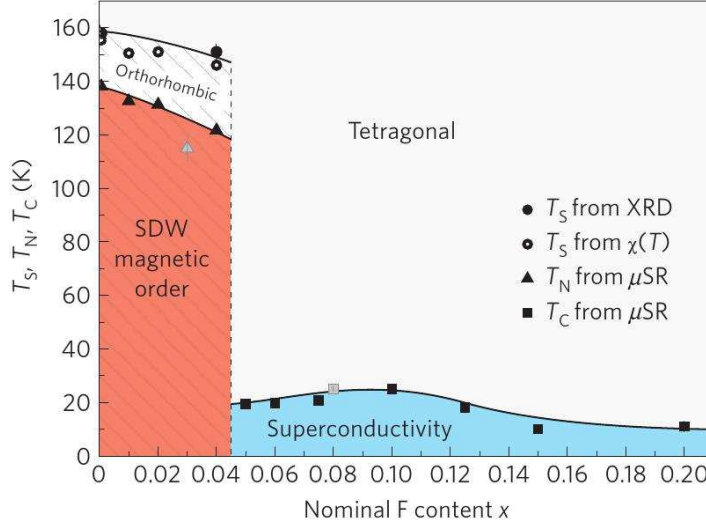


Fig. 1 Electronic phase diagram of $\text{LaFeAsO}_{1-x}\text{F}_x$. The doping dependence of the magnetic and superconducting transition temperatures determined from the μSR experiments. Also shown are the tetragonal-to-orthorhombic structural transition temperatures T_S determined directly from X-ray diffraction and from susceptibility measurements. Reproduced from [22].

Kondrat et al. have focused on the Nernst effect of three samples out of this phase diagram for the doping levels $x = 0, 0.05, 0.1$ [13]. Figure 2 (a) presents the electrical resistivity, $\rho(T)$, of the parent compound LaFeAsO as a function of temperature T [28, 34]. $\rho(T)$ develops a deviation from a standard metallic linear T -dependence near 300 K upon cooling which leads to a maximum at T_s and a subsequent sharp drop with an inflection point at T_N (visible through an inflection point in ρ and hence a sharp peak in $d\rho/dT$) [24, 27, 28, 34, 35]. A further decrease of temperature leads to a minimum of $\rho(T)$ at ~ 90 K followed by a strong low- T upturn. The origin of this quite anomalous temperature dependence of the resistivity is not entirely clear. Qualitatively, it seems straightforward, however, to rationalize the observed anomalies in terms of enhanced scattering at $T > T_s$, presumably arising from fluctuations, and, in the SDW state, a reduced carrier density together with a dramatically reduced carrier scattering rate. In particular, the drastic drop of $\rho(T)$ in the SDW state implies a strong enhancement of the carrier relaxation time. The actual nature of the fluctuations which give rise to the enhanced $\rho(T)$ at $T > T_s$ is uncertain. However, there is strong evidence that SDW fluctuations are present and apparently couple to the charge dynamics. Thermal expansion data reveal an extended fluctuation region in the same regime at $T > T_s$, where the resistivity deviates from linearity [36]. This is corroborated by the predominantly phononic heat conductivity κ of LaFeAsO which exhibits a strong dip-like anomaly at $T \approx T_s$ [28, 35] which also signals that structural fluctuations are relevant. Due to the tight relationship of the low-temperature orthorhombic distortion with the SDW state, magnetic fluctuations are likely to accompany the structural fluctuations at $T > T_s$.

Fig. 2 Normalized resistivity $\rho(T)$ and the derivative $d\rho/dT$ (a) and Nernst coefficient ν (full circles) and $\text{Stan}\theta/B$ (open circles) of LaFeAsO as a function of temperature (b). The solid line is a guide to the eye. Data reproduced from [13, 34].

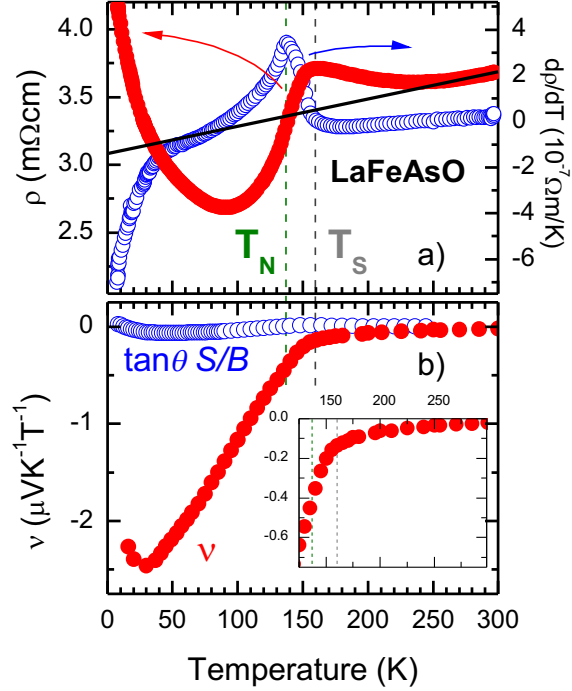
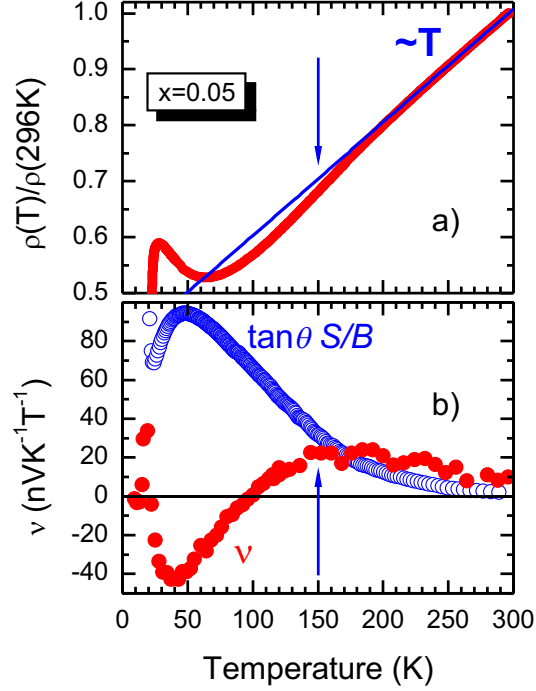


Figure 2b) shows the temperature dependence of the Nernst coefficient $\nu(T)$ of LaFeAsO [13] in direct comparison with the electrical resistivity. $\nu(T)$ is negative over the whole T range. It decreases moderately from $\nu = -0.02 \mu\text{VK}^{-1}\text{T}^{-1}$ at 300 K down to $\nu = -0.2 \mu\text{VK}^{-1}\text{T}^{-1}$ at about 150 K. As can be seen in the figure, at $T \lesssim 150$ K, i.e. almost coinciding with the strong drop in the electrical resistivity upon the onset of SDW order, a large negative contribution becomes apparent. The slope of $\nu(T)$ changes strongly and the Nernst coefficient falls towards a large negative value of $-2.5 \mu\text{VK}^{-1}\text{T}^{-1}$ at around 25 K. Qualitatively, this strong enhancement of the Nernst coefficient should be attributed to the Fermi surface reconstruction that is associated with the SDW phase [7, 13]. The value of the Nernst coefficient in the SDW state is remarkably large, because it is about one order of magnitude larger than that generated by vortex flow in the superconducting samples (see below) or in, e.g., cuprate superconductors [5, 18] which is often considered as a benchmark for a large Nernst effect. Note that a qualitatively similar but quantitatively one order of magnitude smaller impact of SDW order on the Nernst effect has been observed also in CaFe_2As_2 and EuFe_2As_2 by Matusiak et al. [20, 21].

Kondrat et al. have investigated to what extent the 'Sondheimer cancellation' is violated in the SDW phase by comparing the term $\text{Stan}\theta/B$ (which can be easily computed from thermopower, Hall, and resistivity data) [13, 28, 34]. The direct comparison of this quantity with the Nernst coefficient reveals clearly $|\nu| \gg$

Fig. 3 Normalized resistivity $\rho(T)$ (a) and Nernst coefficient v (full circles) and $S \tan \theta / B$ (open circles) of $\text{LaFeAsO}_{1-x}\text{F}_x$ at $x = 0.05$ as a function of temperature (b). The solid line shows a linear fit to the high-temperature resistivity. Arrows mark the onset of non-linearity in the resistivity and of a strong negative contribution to the Nernst coefficient. Data reproduced from [34, 13].



$|S \tan \theta|/B$, i.e. a *severe* violation of the Sondheimer cancellation in the SDW phase (see Figure 2b)).

Superconductivity with rather high critical temperature T_c abruptly emerges in $\text{LaFeAsO}_{1-x}\text{F}_x$ approximately at the doping level $x = 0.05$ [22]. The normal state resistivity $\rho(T)$ drastically changes as compared to that of $\text{LaFeAsO}_{1-x}\text{F}_x$ at $x \leq 0.04$ which still exhibit SDW order [28, 34]. A low- T upturn ($T \lesssim 60$ K) is still present before entering the superconducting state at $T_c \approx 21$ K, which is reminiscent of the low- T upturn of the parent compound. At high temperature, however, the clear features at ~ 150 K of the non superconducting samples have disappeared and ρ increases monotonically for $T \gtrsim 60$ K up to 300 K. Hess et al. have pointed out a surprising feature at intermediate temperature [34]: while $\rho(T)$ becomes linear at $T \gtrsim 250$ K, it drops below the low- T extrapolation of this linearity (cf. Figure 3 (a)). Based on the similarity to the SDW-anomalies in the resistivity of the parent compound, it has been suggested that fluctuations connected to the SDW should still be present, despite the suppression of the actual structural and magnetic transitions [22, 29].

The temperature dependence of the Nernst coefficient of this 'underdoped' sample is reproduced in Figure 3b) [13]. In the superconducting state a strong positive contribution arising from vortex motion is present which extends up to about 40 K. At higher temperature a surprising similarity of $v(T)$ with that of the parent compound becomes apparent: Between 300 K and about 150 K, $v(T)$ is rather weakly

temperature dependent, but at around 150 K the T -dependence changes and a sizable negative contribution leads to a sign change at ~ 100 K and a minimum at ~ 40 K where the positive contribution from vortex motion sets in. Kondrat et al. pointed out that in this low-temperature regime (i.e., $T \lesssim 150$ K) $|v| \approx |S \tan \theta|/B$, i.e. a significant violation of the Sondheimer cancellation is still present. Furthermore, the negative contribution between 40 K and 150 K, despite a strongly reduced magnitude as compared to that of the parent compound is still of similar size as the vortex contribution at low T [13].

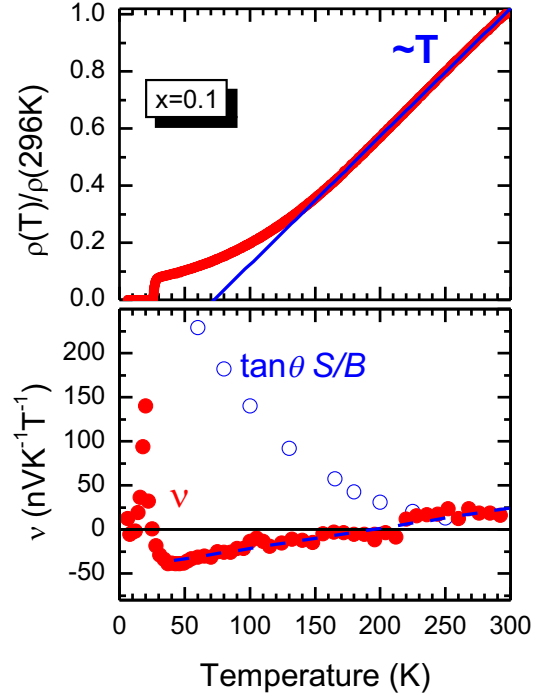
The strong similarity of the anomaly at $T \lesssim 150$ K with the SDW-enhanced Nernst coefficient of the parent compound suggests that SDW order should be also considered in this superconducting sample. However, as already mentioned above, the material exhibits bulk superconductivity, whereas muon spin relaxation (μ SR) and Mössbauer spectroscopy show no trace of magnetic ordering in this T -regime [22, 29]. It seems therefore straightforward to conclude that an SDW precursor, in the form of fluctuations or possibly nematic phases give rise to the enhanced Nernst response [7, 10, 13]. Thus the afore notion, based on the electrical resistivity that SDW fluctuations are present in the normal state of underdoped, superconducting $\text{LaFeAsO}_{1-x}\text{F}_x$ [34] is strongly corroborated. This is consistent with the observation for the parent compound [13] that at $T \gtrsim T_N$, i.e. in a T -range where SDW precursors are truly present [36, 37], the Nernst response is enhanced with a similar magnitude as in the low- T regime of the underdoped material (c.f. inset of Figure 2b)). Note, that the observed negative sign of the SDW-related contribution to the Nernst coefficient unambiguously rules out vortex fluctuations [2, 4, 5] as a thinkable origin since these should give rise to a positive Nernst response.

The enhancement of the doping level to optimal doping $x = 0.1$ leads to drastic changes of both the resistivity and the Nernst effect: in the resistivity, instead of a low- T upturn above T_c , a quadratic increase is observed up to ~ 150 K, i.e. $\rho(T) = \rho_0 + AT^2$ ($\rho_0 = \text{const}$). The resistivity drop at ~ 150 K has practically disappeared and a smooth crossover to a linear high- T behavior is present (cf. Figure 4a)) [34].

In the Nernst response, despite a very similar behavior in the vicinity of T_c and similar magnitude as compared to the underdoped compound a completely different normal state behavior is observed. In the whole normal state at $T \gtrsim 40$ K, $v(T)$ is featureless with a weak positive slope. In particular, no anomaly similar to that of the underdoped material is present. The Sondheimer cancellation is more complete now, i.e. $|v| \ll |S \tan \theta|/B$ is found at low T . Both, the Fermi liquid-like resistivity and rather conventional Nernst effect suggests that $\text{LaFeAsO}_{1-x}\text{F}_x$ at optimal doping displays more normal metallic properties as compared to those of the underdoped and undoped levels. In particular, all features, which could be related to SDW order and or SDW fluctuations are absent.

The doping dependence of the SDW signature in the Nernst response suggests that the material $\text{LaFeAsO}_{1-x}\text{F}_x$ evolves from a very unusual metal at $x = 0$ to a more conventional one at $x = 0.1$, where at $x = 0.05$ the interesting situation of a fluctuating/nematic SDW state appears to be realized. Here, the Nernst effect turns out as a very sensitive probe to this quite subtle state which is not detectable by

Fig. 4 Normalized resistivity $\rho(T)$ (a) and Nernst coefficient v (full circles) and $S \tan \theta / B$ (open circles) of $\text{LaFeAsO}_{1-x}\text{F}_x$ at $x = 0.1$ as a function of temperature (b). The solid line shows a linear fit to the high-temperature resistivity. The dashed line is a guide to the eye. Data reproduced from [34, 13].

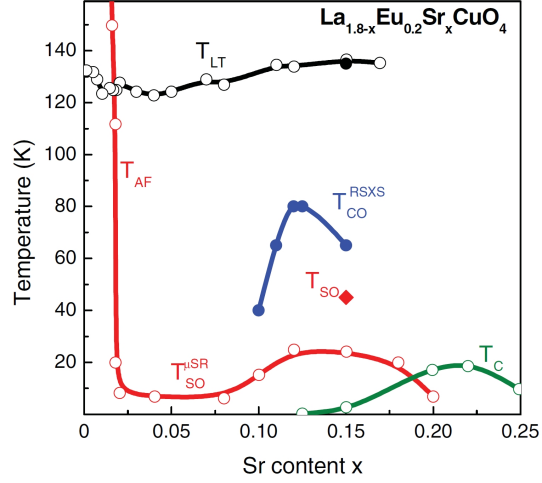


diffraction techniques or local probes such as μSR or Mößbauer spectroscopy [22, 29].

3 Nernst effect and stripe order in the cuprate superconductor $\text{La}_{1.8-x}\text{Eu}_{0.2}\text{Sr}_x\text{CuO}_4$

In cuprate superconductors, the tendency towards the segregation of spins and holes is much under debate with respect to the nature of superconductivity and the pseudogap phase [6, 9, 38, 39, 40, 41, 42, 43, 44]. Clear evidence for *static stripe order* has been observed in materials which are closely related to the fundamental cuprate superconducting system $\text{La}_{2-x}\text{Sr}_x\text{CuO}_4$. Prototype materials exhibiting static stripes are the compounds $\text{La}_{2-x}\text{Ba}_x\text{CuO}_4$ [40, 45, 46, 47, 48, 49] and the closely related $\text{La}_{1.8-x}\text{Eu}_{0.2}\text{Sr}_x\text{CuO}_4$ and $\text{La}_{1.6-x}\text{Nd}_{0.4}\text{Sr}_x\text{CuO}_4$ [38, 50, 51]. In the case of stripe order, these materials exhibit stripe-like arrangements of alternating hole-rich and antiferromagnetic regions, where in all these materials an intimate interplay between structure, stripe order and superconductivity is present. More specifically, bulk superconductivity is suppressed in favor of static stripe order where the latter is stabilized through a particular tilting pattern of the CuO_6 octahedra in the low-temperature tetragonal structural phase (LTT-phase) [23, 38, 47, 52, 53, 54].

Fig. 5 Phase diagram of $\text{La}_{1.8-x}\text{Eu}_{0.2}\text{Sr}_x\text{CuO}_4$ showing transition temperatures for the LTT phase T_{LT} , the anti-ferromagnetic structure T_{AF} , the magnetic stripe order T_{SO} , the stripe-like charge order T_{CO} , and the superconducting transition temperature T_c . Closed circles from resonant soft x-ray scattering (RSXS) experiments [51]. Open circles from Reference [23]. Closed diamond from neutron diffraction data presented in Ref. [60]. Reproduced from [51].



In the prototype stripe ordering compound $\text{La}_{2-x}\text{Ba}_x\text{CuO}_4$ the LTT phase is only present in a limited doping range around $x = 1/8$ [55]. At this very doping level, the LTT phase and therefore static stripe order is present only at relatively low temperature $T \lesssim 55$ K, where the stripe order sets in abruptly directly at the transition to the LTT phase [56, 57]. Recently, very intriguing results for the Nernst effect of this materials have been reported [58], which point to time-reversal symmetry breaking due to the stripe order. The reported onset of a spontaneous Nernst signal related to the stripe order deserves further attention which is, however, out of the scope of this overview.

Concerning the stabilization of the LTT phase, $\text{La}_{1.8-x}\text{Eu}_{0.2}\text{Sr}_x\text{CuO}_4$ is very different as compared to $\text{La}_{2-x}\text{Ba}_x\text{CuO}_4$ and also $\text{La}_{1.6-x}\text{Nd}_{0.4}\text{Sr}_x\text{CuO}_4$. The LTT phase is present at lowest temperature over a wide doping range, see Figure 5. In addition, irrespective of doping, the transition temperature extends up to rather high temperatures $T_{LT} \approx 120 \pm 10$ K, i.e. much higher than in $\text{La}_{2-x}\text{Ba}_x\text{CuO}_4$ and $\text{La}_{1.6-x}\text{Nd}_{0.4}\text{Sr}_x\text{CuO}_4$ where $T_{LT} \approx 55$ K and $T_{LT} \approx 70$ K, respectively [52, 53, 56, 57, 59]. Bulk superconductivity with a considerable critical temperature T_c is suppressed in $\text{La}_{1.8-x}\text{Eu}_{0.2}\text{Sr}_x\text{CuO}_4$ over a wide doping range up to $x \lesssim 0.2$. Around $x = 0.2$ the tilt angle of the octahedra and hence the buckling of the plane which decreases with increasing hole doping becomes smaller than a critical value [23, 54]. At $T > T_{LT}$ the structure enters the low temperature orthorhombic (LTO) phase in which the buckling pattern of the CuO_2 planes does not support static stripe order [23]. At even higher temperatures the structure enters a further tetragonal phase (so-called high temperature tetragonal phase, HTT) at T_{HT} . In the case of $\text{La}_{1.8-x}\text{Eu}_{0.2}\text{Sr}_x\text{CuO}_4$, $T_{HT} > 300$ K, at $x \leq 0.15$ and $T_{HT} \approx 220$ K for $x = 0.2$ [23].

Hess et al. have recently reported the transport properties of $\text{La}_{1.8-x}\text{Eu}_{0.2}\text{Sr}_x\text{CuO}_4$ ($x = 0.04, 0.08, 0.125, 0.15, 0.2$) with a special focus on the Nernst effect in the normal state [14]. Figure 6 presents the temperature dependence of the Nernst coefficient ν of all investigated samples.

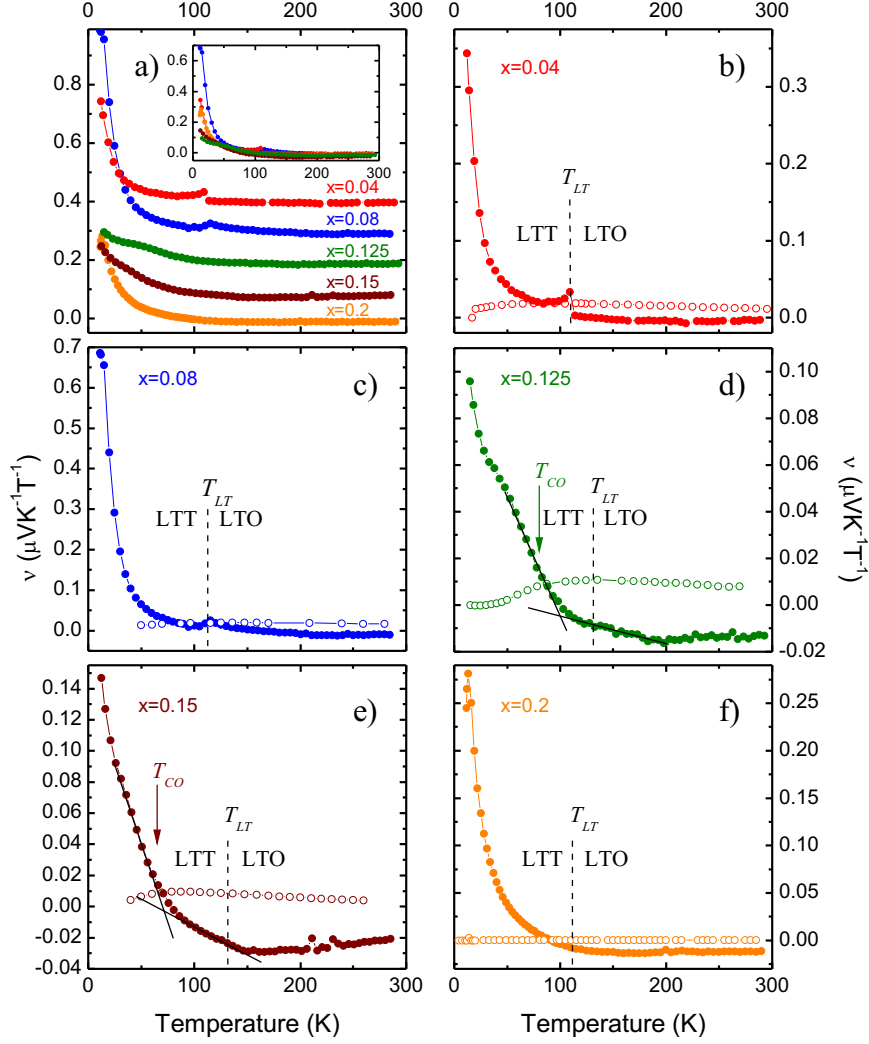


Fig. 6 Nernst coefficient ν of $\text{La}_{1.8-x}\text{Eu}_{0.2}\text{Sr}_x\text{CuO}_4$ ($x = 0.04, 0.08, 0.125, 0.15, 0.2$) as a function of temperature. a) Overview on all data. The presented curves have been shifted for clarity. Inset: all curves at the same scale. b)-f) Temperature dependence of ν (full symbols) and of $\text{Stan } \theta/B$ (open symbols) for each doping level. Solid lines are linear extrapolations of $\nu(T)$ in order to extract T_{ν^*} . Arrows mark the charge stripe ordering temperatures T_{CO} for $x = 0.125, 0.15$ as seen in RSXS experiments [50], see Figure 5. Reproduced from [14].

Panel a) of the figure shows an overview on all data. Clearly, the overall magnitude of the Nernst coefficient is very similar in the temperature range which corresponds to the normal state, i.e. at $T \gtrsim 50$ K. Relatively small anomalies are present in $\nu(T)$ which will be discussed in more detail further below. At lower temperatures ($T \lesssim 50$) all curves strongly increase with falling temperature. However, the mag-

nitude of the increase is quite non-monotonic as a function of doping with a clear minimum at $x = 1/8$. This low-temperature rise in the Nernst coefficient can thus be attributed to fluctuations of the superconducting order parameter which experiences a severe suppression in the presence of stripe order [23], which is strongest at $x = 1/8$.

The individual curves for the Nernst coefficient ν (full symbols) of each doping level are separately shown in panels b) to f) of Figure 6. As was done above for $\text{LaFeAsO}_{1-x}\text{F}_x$, the quantity $S \tan \theta / B$ (open symbols) is displayed as well [14] which allows to judge whether any of the observed anomalies is related to α_{xy} , i.e. a true off-diagonal thermoelectric quantity or to an anomalous behavior in the complementary transport coefficients.

Before discussing the potential effect of stripe order on the Nernst response it is interesting to examine the data with respect to any impact of the structural transition at T_{LT} which is present in all compounds [23, 61]. Indeed, a jump-like anomaly is present at T_{LT} for $x = 0.04$ and $x = 0.08$, where the jump size for the latter is smaller. No anomaly is present at higher doping levels. Interestingly, $S \tan \theta / B$ does not contribute significantly to the observed jumps. This means that the Nernst response, more specifically, α_{xy} , directly couples to structural distortions of the CuO_2 -plane. There is an apparent correlation of the jump size to the degree of buckling of the CuO_2 plane, since concomitantly to the decrease of the jump size (towards its complete disappearance at $x \geq 0.125$) with increasing Sr doping level the tilting angle of the CuO_6 octahedra decreases as well [54]. However, it seems reasonable that not only structural (degree of buckling) but also electronic details (hole content) play a decisive role in this regard because the anomaly at T_{LT} decreases very rapidly with increasing doping.

The closer inspection of the data shown in Figure 6 reveals further interesting features which are clearly discernible at $x = 0.125$ and $x = 0.15$. For $x = 0.125$, two kink-like features are present which deserve closer consideration (see figure 6d). One is located deep in the LTT phase at $T_{V*} \approx 100$ K and is connected with a strong change of slope, the other occurs at much higher temperature $T_V \approx 180$ K, which is in the LTO phase. The measured onset temperatures of the charge stripe and the spin stripe order which are known as $T_{CO} = 80$ K [50, 51] and $T_{SO} \approx 45$ K [23, 60], respectively. These are clearly at much lower temperature than both T_{V*} and T_V , and thus a connection with the observed kinks is not obvious. However, the lower-temperature kink at T_{V*} and the charge stripe ordering temperature T_{CO} , detected by RSXS experiments, occur at a not too different temperature, which brings to mind a possible close connection between both. As all diffraction experiments also the RSXS requires a certain correlation length of the stripe order to be exceeded in order to generate a superlattice reflection. Short range stripe order might already develop at T_{V*} , giving rise to an enhanced Nernst coefficient at this temperature, but are beyond resolution in RSXS. Only at the onset of long range order at T_{CO} RSXS is able to detect the stripe order.

On the other hand, the kink-temperature T_V seems to be too high to account for the stripe ordering phenomena in the LTT phase in an obvious manner. A possible interpretation for the high-temperature anomaly has been suggested by Cyr-

Choinière et al. who speculated that the high temperature kink could mark the onset of stripe fluctuation which could cause a Fermi surface reconstruction [6]. On the other hand, Hess et al. [14] pointed out that one cannot exclude that subtle structural effects unrelated to electronic order are the actual cause of the slight enhancement at T_V . For example, soft phonon type precursors of the LTO \rightarrow LTT transition are known to be ubiquitous in the LTO phase of both $\text{La}_{2-x-y}\text{RE}_y\text{Sr}_x\text{CuO}_4$ (RE=Rare Earth), which undergoes the LTO \rightarrow LTT transition, and $\text{La}_{2-x}\text{Sr}_x\text{CuO}_4$, which remains in the LTO phase down to lowest temperature [62, 63, 64]. In fact, this conjecture is supported by the jump-like response of the Nernst coefficient at T_{LT} for the lower doping levels. It seems noteworthy to mention that Cyr-Choinière et al. reported very similar data for $\text{La}_{1.8-x}\text{Eu}_{0.2}\text{Sr}_x\text{CuO}_4$ at $x = 0.125$ as compared to the data shown in Figure 6. However, their data exhibit a significantly lower $T_V \approx 140$ K (which is very close to the temperature of the structural phase transition T_{LT} and lack a kink at T_{V^*} [6].

The situation at $x = 0.15$ is very similar to that of $x = 0.125$. There, $T_{V^*} \approx 70$ K and $T_V \approx 145$ K with respect to $T_{CO} = 65$ K [50, 51] and $T_{SO} \approx 45$ K [23, 60]. Note that $T_{V^*} \approx T_{CO}$ in this case which corroborates the above conjecture that the kink at T_{V^*} could be related to the formation of static charge stripe order.

Similarly clear anomalies as those seen for $x = 0.125$ and $x = 0.15$ are not discernible at other doping levels. In order to detect a potential anomalous enhancement of the Nernst coefficient due to stripe order, Cyr-Choinière et al. have suggested to plot the quantity v/T versus temperature. This representation relies on the assumption that ordinary normal state quasiparticles should cause a Nernst response which is linear in temperature, when no Fermi surface reconstruction and no contribution from superconductivity are present [6].

Panels a) to e) of Figure 7 display this representation for the afore discussed Nernst effect data of $\text{La}_{1.8-x}\text{Eu}_{0.2}\text{Sr}_x\text{CuO}_4$ [14]. Indeed, at all doping levels up to $x = 0.15$, v/T is linear at high T and deviates from this linearity at a characteristic temperature. This characteristic temperature decreases monotonically upon increasing doping, where for $x = 0.125$ and 0.15 it is identical to that of the high-temperature kink at T_V . One should note that the doping level $x = 0.2$, despite v/T being also linear in T at high temperature, should not be considered in this way since this sample undergoes two structural transitions in the region of interest. One is the LTO \rightarrow LTT transition at $T_{LT} \approx 110$ K, the other is the HTT \rightarrow LTO transition at $T_{HT} \approx 220$ K.

Hess et al. have summarized their findings [14] in the phase diagram shown in Figure 7f). The main finding from the investigated data on $\text{La}_{1.8-x}\text{Eu}_{0.2}\text{Sr}_x\text{CuO}_4$ is the rather good agreement between the lower kink temperature T_{V^*} and the charge stripe ordering temperature T_{CO} for the doping levels $x = 0.125$ and 0.15 , where the stripe order has been experimentally detected by diffraction experiments. Qualitatively, the enhanced v at $T < T_{CO}$ seems consistent with theoretical results by Hackl et al., who calculated the temperature dependence of the quasiparticle Nernst effect for $p = 1/8$ stripe order in a mean field approach [8].

It was further pointed out [14] that the salient, stripe order-induced features are, in fact, very subtle anomalies. To illustrate this, they compared the Nernst coef-

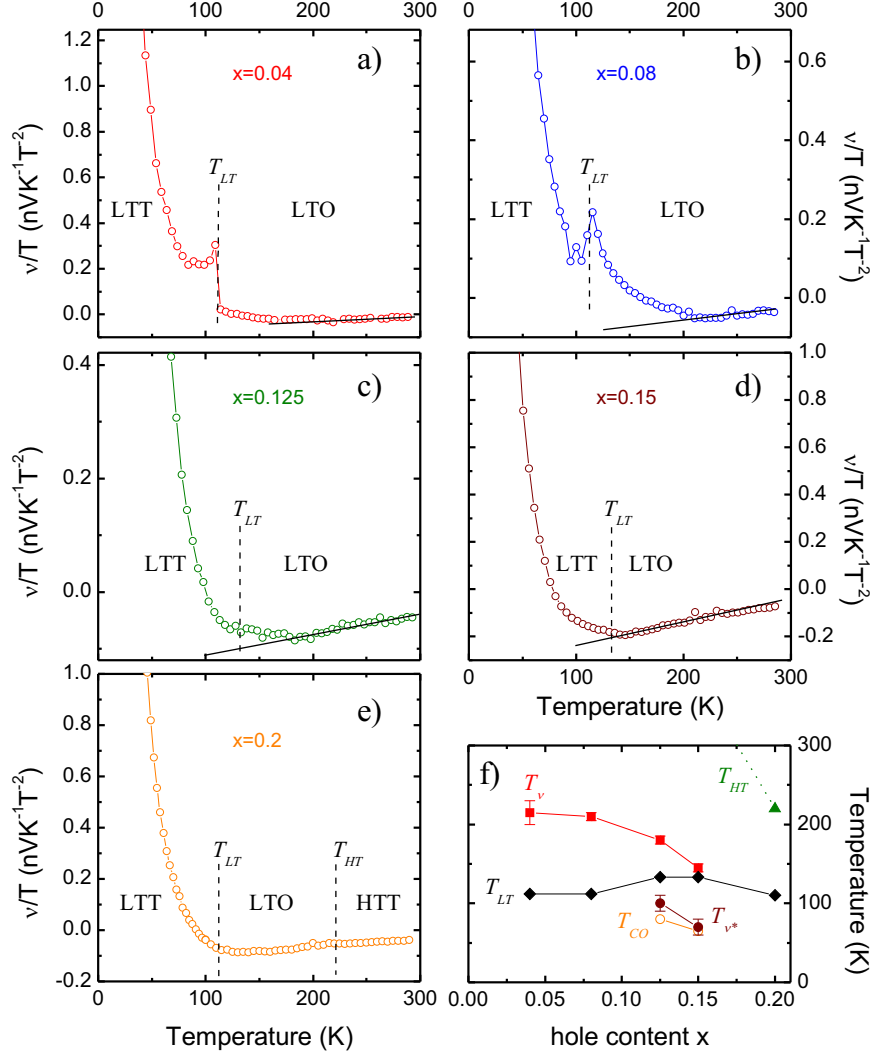


Fig. 7 a)-e) v/T of $\text{La}_{1.8-x}\text{Eu}_{0.2}\text{Sr}_x\text{CuO}_4$ ($x = 0.04, 0.08, 0.125, 0.15, 0.2$) as a function of temperature. Solid lines are linear extrapolations of the high temperature linear behavior of $v(T)$ in order to extract T_v . f) Phase diagram showing T_{LT} (\blacklozenge), T_{HT} (\blacktriangle), T_v (\blacksquare), T_{v^*} (full circles) and T_{CO} (open circles) from RSXS measurements [50, 51]. Reproduced from [14].

ficient of both stripe ordering $\text{La}_{1.8-x}\text{Eu}_{0.2}\text{Sr}_x\text{CuO}_4$ and non-stripe ordering, bulk superconducting $\text{La}_{2-x}\text{Sr}_x\text{CuO}_4$ for the doping levels $x \approx 0.125$ and $x = 0.15$ (see Figure 8). Apparently the Nernst-effect of both variants is very similar in the normal state ($T \gtrsim 60$ K), in particular, in the vicinity of the kink anomalies at T_v and T_{v^*} in the chosen scale, no significant difference is detectable. Strong differences occur only below $T \approx 60$ K where apparently true superconducting fluctuations lead to

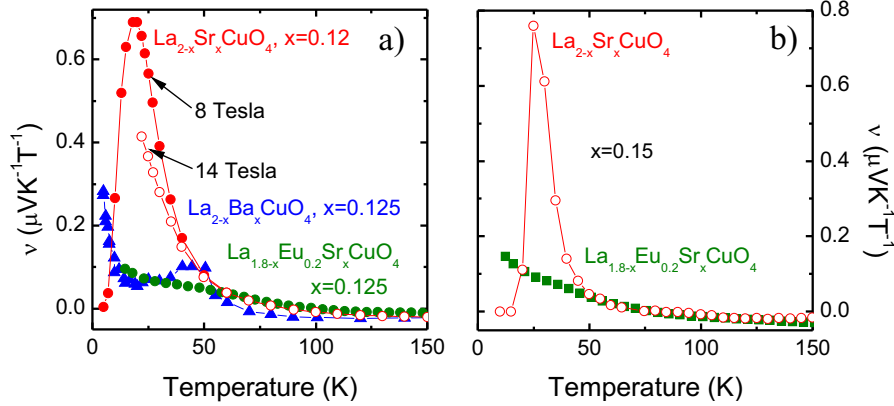


Fig. 8 Nernst coefficient ν of $\text{La}_{2-x}\text{Sr}_x\text{CuO}_4$ (circles), $\text{La}_{1.8-x}\text{Eu}_{0.2}\text{Sr}_x\text{CuO}_4$ (squares) and $\text{La}_{2-x}\text{Ba}_x\text{CuO}_4$ (triangles) as a function of temperature. a) $\text{La}_{1.8-x}\text{Eu}_{0.2}\text{Sr}_x\text{CuO}_4$ and $\text{La}_{2-x}\text{Ba}_x\text{CuO}_4$ at $x = 0.125$ and $\text{La}_{2-x}\text{Sr}_x\text{CuO}_4$ at 0.12 . b) $\text{La}_{1.8-x}\text{Eu}_{0.2}\text{Sr}_x\text{CuO}_4$ and $\text{La}_{2-x}\text{Sr}_x\text{CuO}_4$ at $x = 0.15$. Data taken from [5, 14, 58].

a strong enhancement of ν in $\text{La}_{2-x}\text{Sr}_x\text{CuO}_4$ whereas ν of $\text{La}_{1.8-x}\text{Eu}_{0.2}\text{Sr}_x\text{CuO}_4$ remains much smaller. It is enlightening to compare the findings at $x \approx 0.125$ with the very recent data for $\text{La}_{2-x}\text{Ba}_x\text{CuO}_4$ at this doping level [58] (see Figure 8, left panel). As can be seen in the figure, at $T \gtrsim 60$ K the data for $\text{La}_{2-x}\text{Ba}_x\text{CuO}_4$ are very similar to those of $\text{La}_{2-x}\text{Sr}_x\text{CuO}_4$ and $\text{La}_{1.8-x}\text{Eu}_{0.2}\text{Sr}_x\text{CuO}_4$. In the small interval at $T_{LT} \approx 55$ K $\lesssim T \lesssim 60$ K, i.e., as long as the compound is in the LTO phase and no static stripe order is present, the $\nu(T)$ values are very similar to those of $\text{La}_{2-x}\text{Sr}_x\text{CuO}_4$ and become larger than those of $\text{La}_{1.8-x}\text{Eu}_{0.2}\text{Sr}_x\text{CuO}_4$. At $T \lesssim T_{LT}$, where static stripe order is present, however, the curve drops strongly and becomes very similar to that of $\text{La}_{1.8-x}\text{Eu}_{0.2}\text{Sr}_x\text{CuO}_4$, which is in the stripe-ordered phase in the entire temperature range below $T_{CO} = 80$ K [50, 51].

These observations provide evidence that the magnitude of the Nernst response for static and fluctuating stripes is practically the same (apart from the subtle anomalies at T_V). Theoretical treatments for the Nernst response in the presence of fluctuating stripes are therefore required. On the other hand, the vortex fluctuation scenario attributes the normal state Nernst coefficient in $\text{La}_{2-x}\text{Sr}_x\text{CuO}_4$ and $\text{La}_{2-x}\text{Ba}_x\text{CuO}_4$ at $T \lesssim 120$ K largely to superconducting fluctuations [2, 4, 5, 58]. In particular, for $x = 0.12$ and $x = 0.15$ the onset temperatures of such fluctuations have been inferred from a weak increase of $\nu(T)$ at $T \lesssim 110$ K and $T \lesssim 100$ K, respectively [2, 4, 5, 58]. In view of the similarity between the Nernst effect data in this high-temperature regime for non-stripe ordered $\text{La}_{2-x}\text{Sr}_x\text{CuO}_4$ and $\text{La}_{2-x}\text{Ba}_x\text{CuO}_4$ (at least at $T > T_{LT}$) and stripe ordered $\text{La}_{1.8-x}\text{Eu}_{0.2}\text{Sr}_x\text{CuO}_4$, a theoretical treatment which is based on vortex fluctuation-enhanced Nernst response should explain why in the presence of stripe order, which suppresses bulk superconductivity, the normal state Nernst effect is practically not affected by the stripe order.

4 Conclusion

The above Nernst effect data for the unconventional superconducting systems $\text{LaFeAsO}_{1-x}\text{F}_x$ and $\text{La}_{2-x}\text{Sr}_x\text{CuO}_4$ clearly demonstrate that SDW order (if stripe order of the cuprates is understood as such) has very different impact on this transport quantity, depending on the system. The onset SDW order has a huge effect on the Nernst coefficient of the itinerant antiferromagnet LaFeAsO whereas the effect is tiny in the stripe ordering cuprates [6, 9]. Furthermore, the degree of order has a very different consequence. In $\text{LaFeAsO}_{1-x}\text{F}_x$ at $x = 0.05$ the fluctuating SDW signal is about two orders of magnitude smaller than that of the parent compound where static long range order is present. Despite of this strong suppression, the SDW signal is still substantial and exceeds all effects observed in the cuprates and even typical vortex flow signals [5, 6, 9, 14, 58]. In the cuprates, as was mentioned above, the difference between static and fluctuating stripes is apparently very tiny as can be inferred from the very similar Nernst response of stripe ordered $\text{La}_{1.8-x}\text{Eu}_{0.2}\text{Sr}_x\text{CuO}_4$ and $\text{La}_{2-x}\text{Sr}_x\text{CuO}_4$ for which stripes can be presumed to be fluctuating.

Acknowledgements Support by the Deutsche Forschungsgemeinschaft through the Research Unit FOR538 (Grant No. BU887/4) and the Priority Programme SPP1458 (Grant No. GR3330/2) is gratefully acknowledged. This work would not have been possible without contributions by U. Ammerahl, G. Behr, B. Büchner, A. Revcolevschi, and, in particular, A. Kondrat and E. Ahmed. Furthermore, the author thanks D. Bombor and F. Steckel for proofreading the manuscript.

References

1. K. Behnia, *Journal of Physics: Condensed Matter* **21**, 113101 (2009).
2. Y. Wang, Z.A. Xu, T. Kakeshita, S. Uchida, S. Ono, Y. Ando, N.P. Ong, *Phys. Rev. B* **64**, 224519 (2001).
3. E.H. Sondheimer, *Proc. R. Soc. Lond. A* **193**, 484 (1948).
4. Z.A. Xu, N.P. Ong, Y. Wang, T. Kakeshita, S. Uchida, *Nature* **406**, 486 (2000).
5. Y. Wang, L. Li, N.P. Ong, *Phys. Rev. B* **73**, 024510 (2006).
6. O. Cyr-Choinière, R. Daou, F. Laliberté, D. LeBoeuf, N. Doiron-Leyraud, J. Chang, J.Q. Yan, J.G. Cheng, J.S. Zhou, J.B. Goodenough, S. Pyon, T. Takayama, H. Takagi, Y. Tanaka, L. Taillefer, *Nature* **458**, 743 (2009).
7. A. Hackl, S. Sachdev, *Phys. Rev. B* **79**, 235124 (2009).
8. A. Hackl, M. Vojta, S. Sachdev, *Phys. Rev. B* **81**, 045102 (2010).
9. R. Daou, J. Chang, D. LeBoeuf, O. Cyr-Choinière, F. Laliberté, N. Doiron-Leyraud, B.J. Ramshaw, R. Liang, D.A. Bonn, W.N. Hardy, L. Taillefer, *Nature* **463**, 519 (2010).
10. A. Hackl, M. Vojta, *Phys. Rev. B* **80**, 220514 (2009).
11. P. Fournier, X. Jiang, W. Jiang, S.N. Mao, T. Venkatesan, C.J. Lobb, R.L. Greene, *Phys. Rev. B* **56**, 14149 (1997).
12. P. Li, R.L. Greene, *Phys. Rev. B* **76**, 174512 (2007).
13. A. Kondrat, G. Behr, B. Büchner, C. Hess, *Phys. Rev. B* **83**, 092507 (2011).
14. C. Hess, E. Ahmed, U. Ammerahl, A. Revcolevschi, B. Büchner, *The European Physical Journal - Special Topics* **188**, 103 (2010).
15. R.P. Huebener, A. Seher, *Phys. Rev.* **181**, 701 (1969).
16. F.A. Otter, P.R. Solomon, *Phys. Rev. Lett.* **16**, 681 (1966).

17. S.J. Hagen, C.J. Lobb, R.L. Greene, M.G. Forrester, J. Talvacchio, Phys. Rev. B **42**, 6777 (1990).
18. H.C. Ri, R. Gross, F. Gollnik, A. Beck, R.P. Huebener, P. Wagner, H. Adrian, Phys. Rev. B **50**, 3312 (1994).
19. Z.W. Zhu, Z.A. Xu, X. Lin, G.H. Cao, C.M. Feng, G.F. Chen, Z. Li, J.L. Luo, N.L. Wang, New Journal of Physics **10**, 063021 (2008).
20. M. Matusiak, Z. Bukowski, J. Karpinski, Phys. Rev. B **81**, 020510 (2010).
21. M. Matusiak, Z. Bukowski, J. Karpinski, Phys. Rev. B **83**, 224505 (2011).
22. H. Luetkens, H.H. Klauss, M. Kraken, F.J. Litterst, T. Dellmann, R. Klingeler, C. Hess, R. Khasanov, A. Amato, C. Baines, M. Kosmala, O.J. Schumann, M. Braden, J. Hamann-Borrero, N. Leps, A. Kondrat, G. Behr, J. Werner, B. Büchner, Nat Mater **8**, 305 (2009).
23. H.H. Klauss, W. Wagener, M. Hillberg, W. Kopmann, H. Walf, F.J. Litterst, M. Hücker, B. Büchner, Phys. Rev. Lett. **85**, 4590 (2000).
24. Y. Kamihara, T. Watanabe, M. Hirano, H. Hosono, J. Am. Chem. Soc. **130**, 3296 (2008).
25. Z.A. Ren, W. Lu, J. Yang, W. Yi, X.L. Shen, Z.C. Li, G.C. Che, X.L. Dong, L.L. Sun, F. Zhou, Z.X. Zhao, Chin. Phys. Lett. **25**, 2215 (2008).
26. C. de la Cruz, Q. Huang, J.W. Lynn, J. Li, W.R. II, J.L. Zarestky, H.A. Mook, G.F. Chen, J.L. Luo, N.L. Wang, P. Dai, Nature **453**, 899 (2008).
27. H.H. Klauss, H. Luetkens, R. Klingeler, C. Hess, F.J. Litterst, M. Kraken, M.M. Korshunov, I. Eremin, S.L. Drechsler, R. Khasanov, A. Amato, J. Hamann-Borrero, N. Leps, A. Kondrat, G. Behr, J. Werner, B. Büchner, Phys. Rev. Lett. **101**, 077005 (2008).
28. A. Kondrat, J.E. Hamann-Borrero, N. Leps, M. Kosmala, O. Schumann, A. Köhler, J. Werner, G. Behr, M. Braden, R. Klingeler, B. Büchner, C. Hess, Eur. Phys. J. B **70**, 461 (2009).
29. N. Qureshi, Y. Drees, J. Werner, S. Wurmehl, C. Hess, R. Klingeler, B. Büchner, M.T. Fernández-Díaz, M. Braden, Phys. Rev. B **82**, 184521 (2010).
30. A.J. Drew, C. Niedermayer, P.J. Baker, F.L. Pratt, S.J. Blundell, T. Lancaster, R.H. Liu, G. Wu, X.H. Chen, I. Watanabe, V.K. Malik, A. Dubroka, M. Rossle, K.W. Kim, C. Baines, C. Bernhard, Nat Mater **8**, 310 (2009).
31. N. Ni, S.L. Bud'ko, A. Kreyssig, S. Nandi, G.E. Rustan, A.I. Goldman, S. Gupta, J.D. Corbett, A. Kracher, P.C. Canfield, Phys. Rev. B **78**, 014507 (2008).
32. P. Prelovšek, I. Sega, T. Tohyama, Physical Review B (Condensed Matter and Materials Physics) **80**, 014517 (2009).
33. P. Prelovšek, I. Sega, Phys. Rev. B **81**, 115121 (2010).
34. C. Hess, A. Kondrat, A. Narduzzo, J.E. Hamann-Borrero, R. Klingeler, J. Werner, G. Behr, B. Büchner, EPL (Europhysics Letters) **87**, 17005 (2009).
35. M.A. McGuire, A.D. Christianson, A.S. Sefat, B.C. Sales, M.D. Lumsden, R. Jin, E.A. Payzant, D. Mandrus, Y. Luan, V. Keppens, V. Varadarajan, J.W. Brill, R.P. Hermann, M.T. Sougrati, F. Grandjean, G.J. Long, Physical Review B (Condensed Matter and Materials Physics) **78**, 094517 (2008).
36. L. Wang, U. Köhler, N. Leps, A. Kondrat, M. Nale, A. Gasparini, A. de Visser, G. Behr, C. Hess, R. Klingeler, B. Büchner, Phys. Rev. B **80**, 094512 (2009).
37. Y. Nakai, K. Ishida, Y. Kamihara, M. Hirano, H. Hosono, Journal of the Physical Society of Japan **77**, 073701 (2008).
38. J.M. Tranquada, B.J. Sternlieb, J.D. Axe, Y. Nakamura, S. Uchida, Nature **375**, 561 (1995).
39. S.A. Kivelson, E. Fradkin, V.J. Emery, Nature **393**, 550 (1998).
40. J.M. Tranquada, H. Woo, T.G. Perring, H. Goka, G.D. Gu, G. Xu, M. Fujita, K. Yamada, Nature **429**, 534 (2004).
41. V. Hinkov, S. Pailhes, P. Bourges, Y. Sidis, A. Ivanov, A. Kulakov, C.T. Lin, D.P. Chen, C. Bernhard, B. Keimer, Nature **430**, 650 (2004).
42. V. Hinkov, P. Bourges, S. Pailhes, Y. Sidis, A. Ivanov, C.D. Frost, T.G. Perring, C.T. Lin, D.P. Chen, B. Keimer, Nat Phys **3**, 780 (2007).
43. Y. Kohsaka, C. Taylor, K. Fujita, A. Schmidt, C. Lupien, T. Hanaguri, M. Azuma, M. Takano, H. Eisaki, H. Takagi, S. Uchida, J.C. Davis, Science **315**, 1380 (2007).
44. V. Hinkov, D. Haug, B. Fauqu, P. Bourges, Y. Sidis, A. Ivanov, C. Bernhard, C.T. Lin, B. Keimer, Science **319**, 597 (2008).

45. M. Fujita, H. Goka, K. Yamada, J.M. Tranquada, L.P. Regnault, Phys. Rev. B **70**, 104517 (2004).
46. M. Hückler, M. v. Zimmermann, M. Debessai, J.S. Schilling, J.M. Tranquada, G.D. Gu, Phys. Rev. Lett. **104**, 057004 (2010).
47. J.M. Tranquada, G.D. Gu, M. Hückler, Q. Jie, H.J. Kang, R. Klingeler, Q. Li, N. Tristan, J.S. Wen, G.Y. Xu, Z.J. Xu, J. Zhou, M. v. Zimmermann, Phys. Rev. B **78**, 174529 (2008).
48. J. Wen, Z. Xu, G. Xu, J.M. Tranquada, G. Gu, S. Chang, H.J. Kang, Phys. Rev. B **78**, 212506 (2008).
49. G. Xu, J.M. Tranquada, T.G. Perring, G.D. Gu, M. Fujita, K. Yamada, Phys. Rev. B **76**, 014508 (2007).
50. J. Fink, E. Schierle, E. Weschke, J. Geck, D. Hawthorn, V. Soltwisch, H. Wadati, H.H. Wu, H.A. Dürr, N. Wizen, B. Büchner, G.A. Sawatzky, Phys. Rev. B **79**, 100502 (2009).
51. J. Fink, V. Soltwisch, J. Geck, E. Schierle, E. Weschke, B. Büchner, Phys. Rev. B **83**, 092503 (2011).
52. B. Büchner, M. Braden, M. Cramm, W. Schlabitz, O. Hoffels, W. Braunisch, R. Müller, G. Heger, D. Wohlleben, Physica C: Superconductivity **185-189**, 903 (1991).
53. B. Büchner, M. Cramm, M. Braden, W. Braunisch, O. Hoffels, W. Schnelle, R. Müller, A. Freimuth, W. Schlabitz, G. Heger, D.I. Khomskii, D. Wohlleben, Europhys. Lett. **21**, 953 (1993).
54. B. Büchner, M. Breuer, A. Freimuth, A.P. Kampf, Phys. Rev. Lett. **73**, 1841 (1994).
55. J.D. Axe, A.H. Moudden, D. Hohlwein, D.E. Cox, K.M. Mohanty, A.R. Moodenbaugh, Y. Xu, Phys. Rev. Lett. **62**, 2751 (1989).
56. M. Hückler, M. v. Zimmermann, G.D. Gu, Z.J. Xu, J.S. Wen, G. Xu, H.J. Kang, A. Zheludev, J.M. Tranquada, Phys. Rev. B **83**, 104506 (2011).
57. S.B. Wilkins, M.P.M. Dean, J. Fink, M. Hückler, J. Geck, V. Soltwisch, E. Schierle, E. Weschke, G. Gu, S. Uchida, N. Ichikawa, J.M. Tranquada, J.P. Hill, Phys. Rev. B **84**, 195101 (2011).
58. L. Li, N. Alidoust, J.M. Tranquada, G.D. Gu, N.P. Ong, Phys. Rev. Lett. **107**, 277001 (2011).
59. J.M. Tranquada, J.D. Axe, N. Ichikawa, Y. Nakamura, S. Uchida, B. Nachumi, Phys. Rev. B **54**, 7489 (1996).
60. M. Hückler, G. Gu, J. Tranquada, M. Zimmermann, H.H. Klauss, N. Curro, M. Braden, B. Büchner, Physica C: Superconductivity **460-462**, 170 (2007).
61. C. Hess, B. Büchner, U. Ammerahl, A. Revcolevschi, Phys. Rev. B **68**, 184517 (2003).
62. L. Pintschovius, Festkörperprobleme **30**, 183 (1990).
63. J.L. Martínez, M.T. Fernández-Díaz, J. Rodríguez-Carvajal, P. Odier, Phys. Rev. B **43**, 13766 (1991).
64. B. Keimer, R.J. Birgeneau, A. Cassanho, Y. Endoh, M. Greven, M.A. Kastner, G. Shirane, Z. Phys. B **91**, 373 (1993).